Supporting Information

Experimental Section

Materials: Graphite was purchased from Sinopharm Chemical Reagent (Shanghai, China). $AgNO_3$ (99.9995%), $Na_2S_2O_8$, ascorbic acid (AA), Poly (allyl amine hydrochloride) (PAH, MW=60000), 1-Ethyl-3(3-dimethylaminopropyl) carbodiimide hydrochloride (EDC) and N-Hydroxysulfosuccinimide sodium (sulfo-NHS) were purchased from Alfa Aesar used without further purification. Bovine serum albumin (BSA) was provided by Sangon (Shanghai, China). All other chemicals were purchased from Sigma–Aldrich and used as supplied. All aqueous solutions were prepared with ultra-pure water (18.2 MΩ cm, Milli-Q, Millipore).

Apparatus and Characterizations: UV absorbance measurements were carried out on a JASCO v-550 UV-vis spectrophotometer with a Peltier temperature control accessory. Fluorescence spectra were measured on a JASCO FP-6500 spectrofluorometer equipped with a temperature-controlled water bath. All the spectra were recorded with a 1.0 cm path length cell. FT-IR characterization was carried out on a BRUKE Vertex 70 FT-IR spectrometer. The samples were thoroughly ground with exhaustively dried KBr. Atomic force microscopy (AFM) measurements were performed using Nanoscope V multimode atomic force microscope (Veeco Instruments, USA). Transmission electron microscopic (TEM) images were recorded using a FEI TECNAI G2 20 high-resolution transmission electron microscope operating at 200 KV. For visualization by TEM, samples were prepared by dropping solutions of production on a copper grid. X-ray photoelectron spectroscopy (XPS) spectra were obtained with an ESCALAB Thermal 250 instrument and monochromatic Mg-Ka (E=1253.6 eV) was used for photoexcitation. Photographs were taken with a Canon IXUS 900Ti digital camera.

Electrochemical Measurements: Cyclic voltammetry (CV) measurements were carried out with a CHI 660B Electrochemistry Workstation (CHI, USA) in 10 mM $K_3[Fe(CN)_6]$, 1 M KCl and 100 mM phosphate buffered saline (PBS, pH 7.5) solution, 100 mM $Na_2S_2O_8$ with a conventional three-electrode system comprised of a platinum wire as the auxiliary electrode, an Ag/AgCl as the reference electrode and the modified GCE used as working electrode. EIS was performed using CHI 660B in 100 mM PBS containing 10 mM $K_3[Fe(CN)_6]/K_4[Fe(CN)_6]$ (1:1) mixture with 1 M KCl as the supporting electrolyte. The impedance spectra were recorded within the frequency range of 10^{-2}-10^5 Hz. The amplitude of the applied sine wave potential in each case was 5 mV. ECL measurements were carried out with a BPCL-2-TGC Ultra Weak Luminescence Analyzer (Beijing, China) with a photomultiplier tube voltage set at 900 V. The total volume of the reaction medium was 2 mL. During measurements, potential supplied by the CHI 660B Electrochemistry Workstation was applied to the C-dots@Ag/GP-modified glassy carbon electrode (C-dots@Ag/GP/GCE) by a CV technique with a potential range from 0 to -2.0 V at a scan rate of 50 mV/s. At the same time, the ECL emission was recorded in 100 mM PBS (pH 7.5) containing 100 mM $Na_2S_2O_8$ as coreactant by the BPCL-2-TGC Ultra Weak Luminescence Analyzer. The ECL spectrum was obtained by collecting the ECL data at -1.90 V during a cyclic potential sweep with 15 pieces of filters at 620, 605, 590, 575, 555, 535, 520, 505, 490, 475, 460, 440, 425, 412 and 400 nm. Their thickness and transparent efficiency were 2 mm and 88%, respectively.

Synthesis of PAH-Functionalized Graphene (GP): Graphene oxide (GO) was synthesized from graphite by modified Hummers method.[1] GP was prepared by following the procedures as we previously described.[2] Briefly, a solution of 20 mg of the graphene oxides, 100 mg of PAH, and 100 mg of KOH in 50 mL of H_2O was kept at 70 ℃ for 24 h under vigorously stirring. Then 10 mL of 1M $NaBH_4$ solution was added, and the reaction was kept on at 70 ℃ for 2 h. After that, the GP was collected and purified by centrifugation and adequately washed with water several times to remove the impurities and the excess of PAH by physical absorption.

Synthesis of Carbon Nanodots: Carbon nanodots were prepared by adopting a procedure reported in the literature.[3] Briefly, Candle soot was collected by putting a piece of glass plate on top of burning unscented candles. 100 mg of candle soot was mixed with 20 mL of 5 M nitric acid in a 50 mL three-necked flask. The mixture was then refluxed for 12 h with magnetic stirring. After cooling down to room temperature, the black solution was centrifuged at 12,000 rpm for 30 min. The fluorescent C-dots supernatant was collected, neutralized by Na_2CO_3, and extensively dialyzed against Millipore 18.2 MΩ cm water through a dialysis membrane (3500 MWCO). The C-dots were then concentrated by evaporation and dried under vacuum.

Deposition Silver Nanostructures on Carbon Nanodots: C-dots, obtained from the combustion soot of candles, contained abundant carboxylic moieties which were suitable for metal ion Ag^+ bounding by ion exchange or coordination reactions.[4] Upon the addition of the reducing agent ascorbic acid, silver ions were reduced to silver atoms and subsequently served as the nucleation seeds for the growth of metal nanostructures on the surface of C-dots. The procedure of synthesizing C-dots@Ag was followed by the literature with some modification.[4] In a typical reaction, 0.1 mg C-dots was dissolved in 1mL of water. Then 125 μL $AgNO_3$ at a concentration of 4 mg/mL was added into the above solution under magnetic stirring overnight. Next, the calculated amount of ascorbic acid was added in a dropwise fashion under ultrasonication. The color of the solution gradually changed from light brown to dark red, which demonstrated the formation of silver nanostructures on C-dots surface. Excessive salts were moved by centrifugation and the obtained nanocomposite was dispersed in water.

Electrode Modification and ECL Detection of Cancer Cells: The glassy carbon electrodes (GCE, ø=3 mm, CHI) were polished successively with 1.0, 0.3, and 0.05 μm alumina (Buhler) and sonicated for 3 min before modification. A 10-μL GP solution was dropped on the pretreated GCE and dried at room temperature. After washed by 100 mM PBS (pH=7.5) solution 10 μL of C-dots@Ag nanocomposite was dropped on the electrode surface and kept under ambient temperature, then washed by PBS again. Subsequently, the fabricated electrode was immersed into 1 mL cysteine solution with the concentration of 0.02 M and stored in 4 ℃ fridge for 20h. On the same time, the carboxylic groups of FA were firstly activated in the activation solution (10 mM EDC and 25 mM NHS in MES buffer) overnight. The activated folic acid was immediately dropped on the cysteine modified electrode surface and then incubated for 4h. Unconjugated FA was removed by washing the electrode surface with buffer solution. The GP/C-dots@Ag/Cys/FA electrode was immersed into BSA (0.1%, w/v) for 1 h at room temperature to block the nonspecific binding sites, and then washed carefully with PBS. The modified electrodes were stored in air prior to use. The ECL detection was achieved as following: the fabricated electrodes were dipped into a suspension of Hela cells (500 μL) at a certain concentration and incubated at

37 ℃ for 1 h. After carefully rinsing with PBS to remove the non-captured cells, the electrodes were used for subsequent assays. The modified electrodes were in contact with 0.1 M PBS (pH 7.5) containing 0.1 M $Na_2S_2O_8$ and scanned from 0 to -2.0 V. The ECL signals related to the different cancer cells concentrations were measured. The ECL emission was detected with a BPCL-2-TGC Ultra Weak Luminescence Analyzer using a three-electrode system.

Cell Culture and Treatment: The human cervical cancer cells (HeLa), human breast cancer cells (MCF-7) and the mouse fibroblasts cells (NIH-3T3, used as negative control) were grown in flasks in RPMI 1640 medium supplemented with 10% fetal bovine serum, penicillin, and streptomycin (100 μgmL^{-1}) in a 5% CO_2-humidified chamber at 37 ℃. After cultured for 72 h, the cells were collected and separated from the medium by centrifugation at 1000 rpm for 5 min, then washed twice with the sterile PBS (pH 7.2). The cell sediment was re-suspended in the HEPES buffer (25 mM HEPES, 200 mM NaCl, 20 mM KCl) to obtain a homogeneous cell suspension. Cell number was determined using a Petroff-Hausser cell counter. For control experiment, cells in 24 well plate were firstly treated with 200 $\mu g\ mL^{-1}$ FA in IMDM medium for 30 min and then incubated on the electrode surface.[2] For the fluorescence microscope images, the clean glass slides was modified as the same as electrode. The modified slides were immersed into 1×10^5 cells/mL of different cell lines suspension containing RPMI 1640 medium supplemented with 10% fetal bovine serum, penicillin, and streptomycin (100 $\mu g\ mL^{-1}$) in a 5% CO_2-humidified chamber at 37 ℃. After the cancer cells were cultured for 1h, the glass slides were washed by PBS to remove the non-captured cells and then the images of cancer cells on GP/C-dots@Ag/Cys/FA/BSA modified film were stained by AO fluorescent dye for 10 min. Cells were viewed using an Olympus BX-51 optical system microscope (Tokyo, Japan) at 200× magnification with a blue filter. Pictures were taken with an Olympus digital camera.

Supporting Figures

Characterization of the Synthesized GP and C-dots@Ag Nanocomposite

The covalently grafted PAH onto graphene was first characterized by FT-IR measurements (Fig. S1A). The strong CH_2 (~2900 cm-^{1}) and N-H (~3400 cm^{-1}) vibrations, and a characteristic C–N stretch mode (1310 cm^{-1}, ν C–N binding with an aromatic ring) confirmed that the PAH had been covalently grafted to the graphene sheet successfully.[2] TEM images showed that GP surface had a wrinkling paper-like structure and dispersed separately without the aggregation (Fig. S1B). Furthermore, AFM (Fig. S1 C-D) also showed that GP sample separated well with the average topographic height of ca.2.7 nm, which further indicated the existence of PAH on graphene surface.[2]

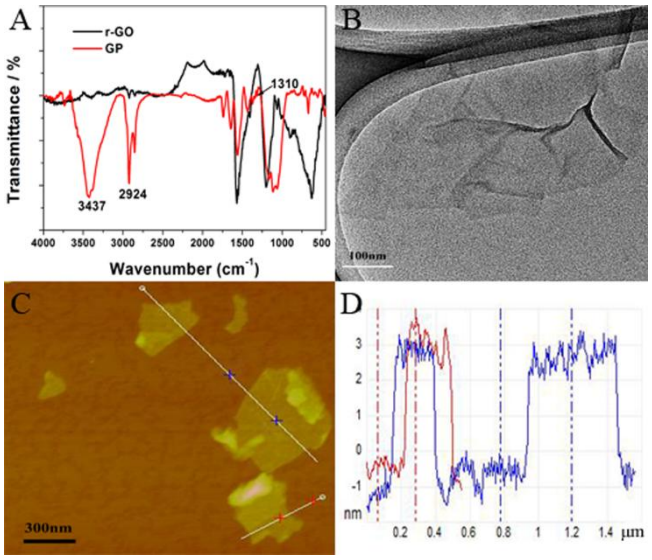

Fig. S1 FT-IR spectra (A), TEM(B) and AFM (C) image of GP, D is the height profile along the line in (C).

As shown in Fig. S2A, TEM studies indicated that the C-dots were mostly of spherical shape and dispersed rather evenly on the grid surface. The lattice planes could be identified with a spacing of 0.211 nm by using HRTEM (Fig. S2B). According to previous studies, this might attribute to the (103) diffraction plane of diamond-like (sp^3) carbon and to the (102) lattice of graphitic (sp^2) carbon.[4] The presence of carboxylic groups on the surface of C-dots was supported by the FT-IR spectrum (Fig. S3). It's suitable for silver ions attachment as the metal ions most likely bound to the peripheral carboxylic moieties by ion exchange or coordination reactions. After reduced by ascorbic acid, the colour of the solution gradually changed from light brown to dark red, which demonstrated the formation of silver nanostructures on C-dots surface (Fig. S4 inset). The size of C-dots@Ag nanocomposite was obviously lager than pure C-dots (Fig. S2C) and the lattice fringes of about 0.233 nm and 0.211 nm might be ascribed to Ag (111) and carbon, respectively (Fig. S2D), consistent with AFM measurements (Fig. S4).

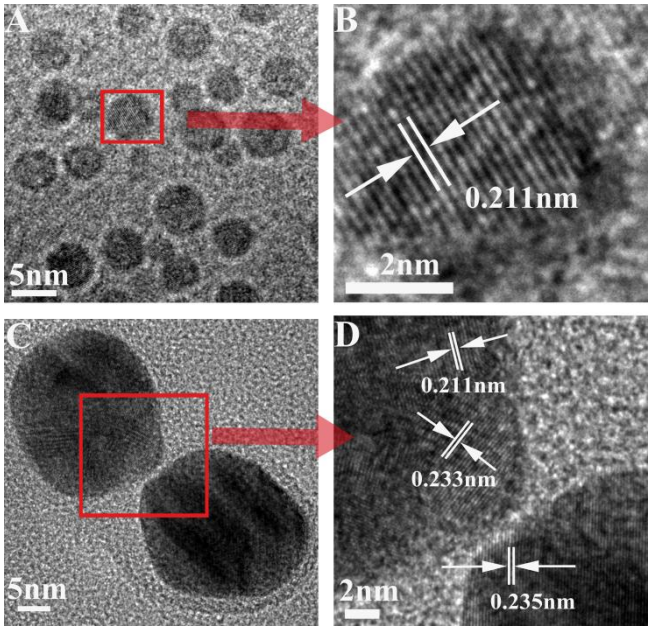

Fig. S2 Representative TEM micrographs of C-dots (A) and C-dots@Ag nanocomposite (C), the insets are corresponding histograms of the overall particle size distribution. The crystalline lattices were identified in the respective HRTEM images for C-dots (B) and C-dots@Ag nanocomposite (D).

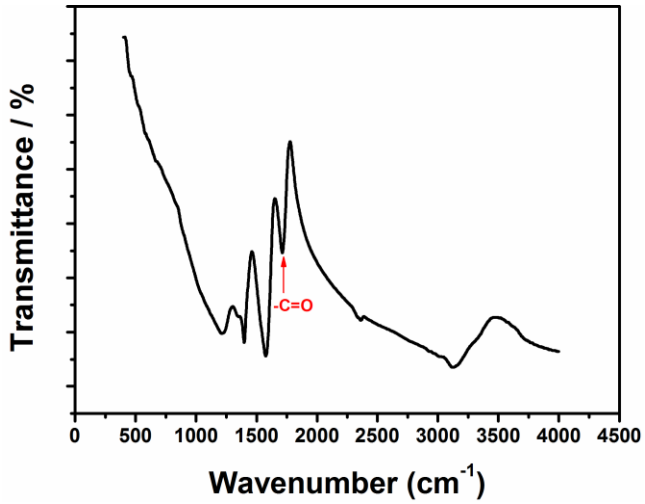

Fig. S3 FT-IR spectrum of C-dots.

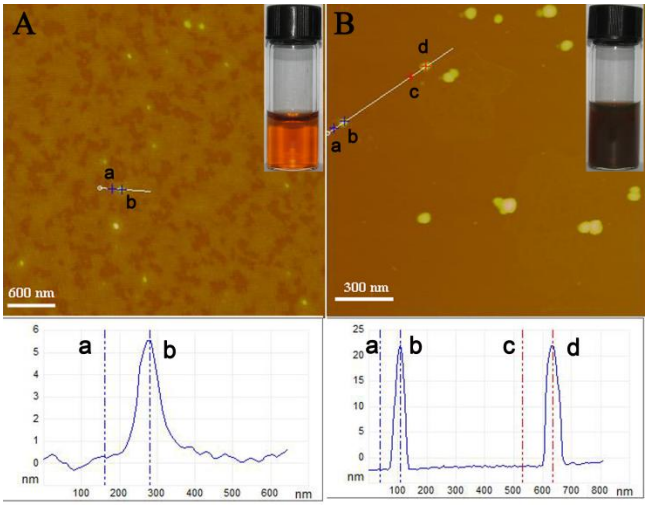

Fig. S4 AFM images of C-dots (A) (inset: image of water dispersion of C-dots) and C-dots@Ag (B) (inset: image of water dispersion of C-dots@Ag).

The surface composition and element analysis for the overall composition of the resultant nanodots were characterized by X-ray photoelectron spectroscopy (XPS). The XPS spectrum of C-dots showed three peaks at 284.1 eV, 400.5 eV and 530.5 eV, which were attributed to C1s, N1s and O1s, respectively. Another peak at 496.8 eV associated with Na was also observed. (Fig. S5A) The XPS measurement showed the C-dots were mainly composed of two elements, C and O; the limited amount of N and Na elements might come from the HNO_3 and Na_2CO_3 during the acid treated and alkali neutralized procession. The high resolution C1s spectrum of the C-dots (Fig. S5B) further supported the presence of Oxygen-rich groups, such as C-O (286.4 eV), C=O (288.1 eV) and O-C=O (289 eV),[5] which was consistent with the FT-IR spectrum (Fig. S3). After addition of silver ions and ascorbic acid reduction, the Ag3d and Ag3p peak were observed in XPS and the content of C=O and O-C=O groups were obviously decreased (Fig. S5C-D). Furthermore, a strong surface plasmon resonance of Ag nanoparticles at 436 nm in the UV-visible absorption spectrum (Fig. S6A) and the quenching-effect of transmission metals in fluorescence spectra (Fig. S6B) also indicated the formation of C-dots@Ag nanostructures.

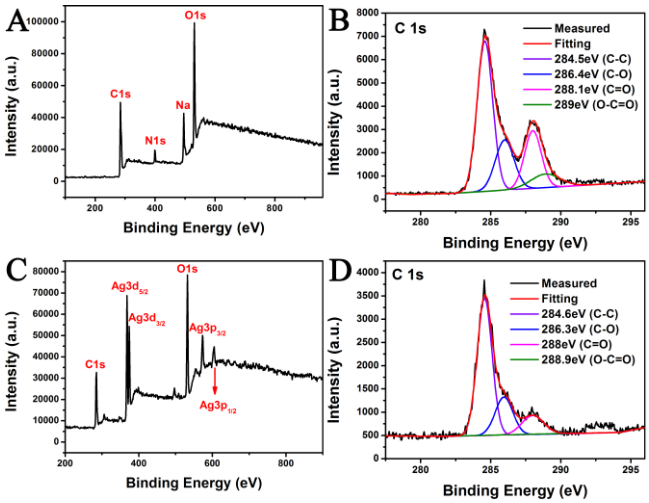

Fig. S5 XPS spectra of C-dots (A) and C-dots@Ag (C); High-resolution XPS scan of C1s of C-dots (B) and C-dots@Ag (D).

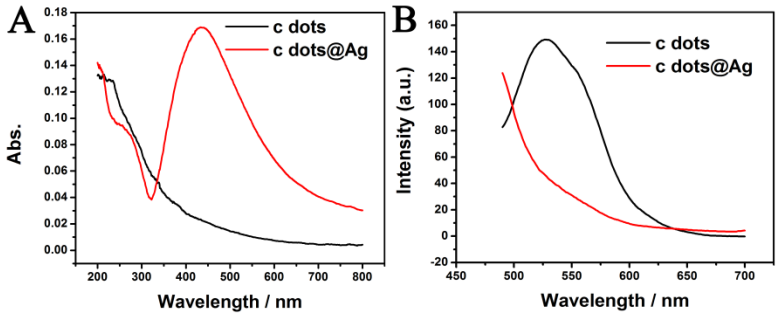

Fig. S6 UV-vis absorption (A) and photoluminescence (B) spectra of C-dots and C-dots@Ag.

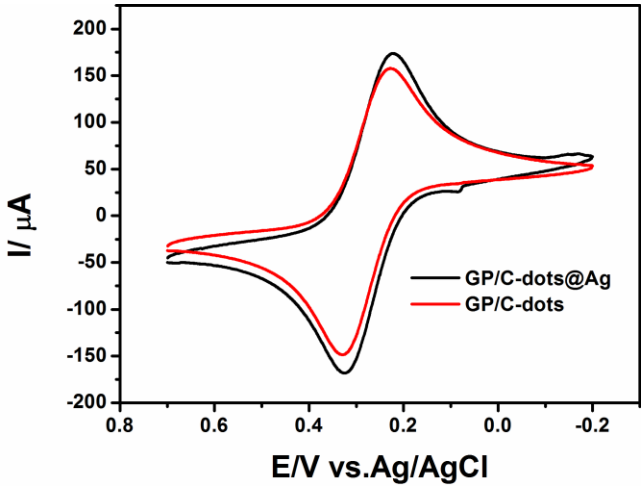

Fig. S7 Cyclic voltammograms (CVs) of GP/C-dots@Ag and GP/C-dots.

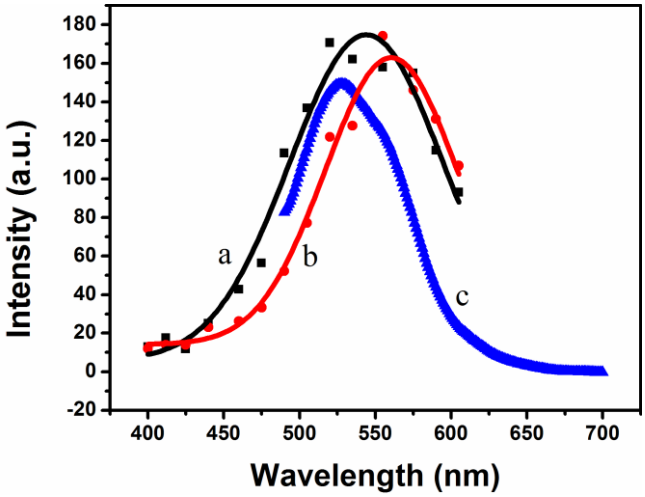

Fig. S8 Electrochemiluminescence (ECL) spectra of C-dots@Ag (a) and C-dots (b); PL spectrum of C-dots (c). The maximum emission wavelength of the coreactant ECL signal for C-dots was at 560 nm, which was red-shift from that of PL maximum (530 nm). This substantial red shift might indicate that surface states on the nanocrystals (NCs) played important role in the electrochemistry and ECL process; This was also observed in the previous experiments with carbon, Si, and Ge nanocrystals (NCs).[6-8] Since charge injection into the NCs generally occurs via surface states, ECL is more sensitive to the surface energies than PL, which occurs mainly from the interior of the NCs. Thus completely passivated C-dots by silver in our experiment showed that ECL spectrum was similar to the PL spectrum, which was consistent with previous report.[9-10] This indicated that silver passivation changed the surface state of C-dots.

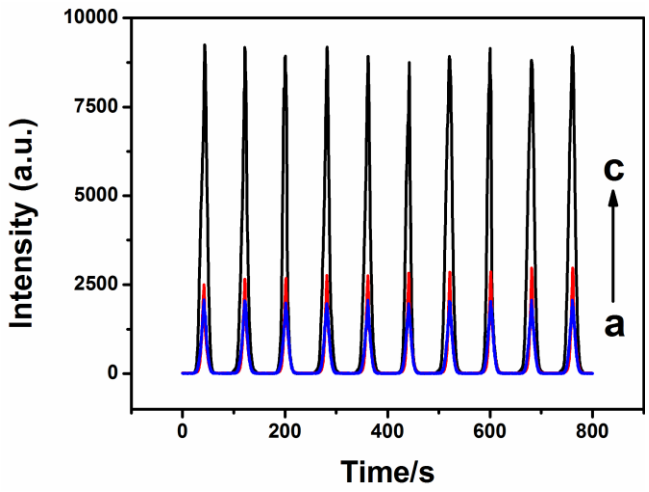

Fig. S9 Continuous cyclic ECL scans of C-dots (a), C-dots treated by AA (b), C-dots@Ag (c) on GCE in 100mM PBS (pH=7.5) solution containing 100mM $Na_2S_2O_8$.

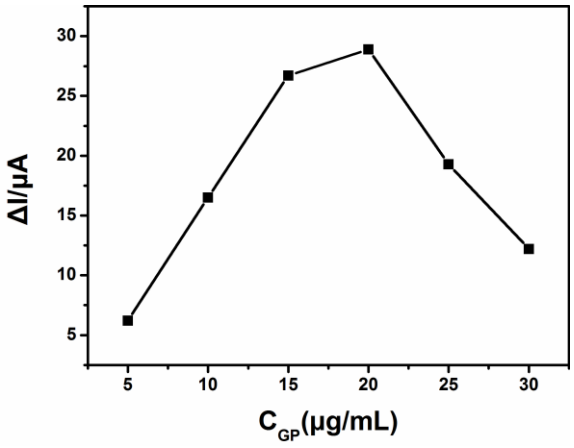

Fig. S10 The optimized amount of GP used for electrode modification.

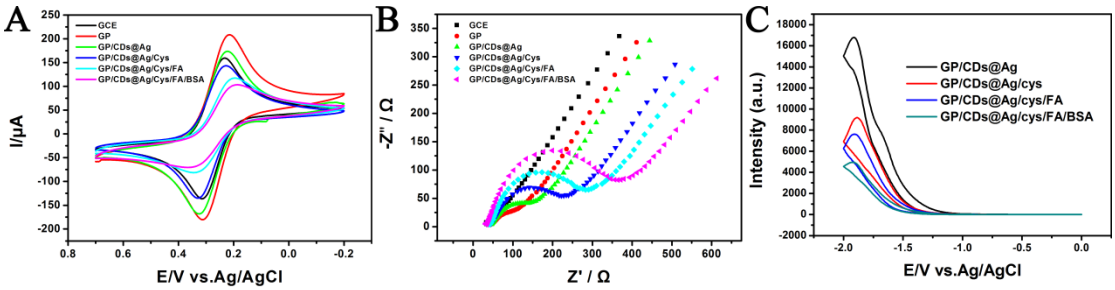

Fig. S11 Cyclic voltammetry (CV) (A) and Electrochemical impedance spectroscopy (EIS) (B) of bare GC electrode (black line); GP modified GCE (GP/GCE) (red line); C-dots@Ag conjugated to the GP/GCE surface (GP/C-dots@Ag) (green line); Cysteine modified on GP/C-dots@Ag (GP/C-dots@Ag/Cys) (dark blue line); FA linked to the cysteine on the electrode surface (GP/C-dots@Ag/Cys/FA) (light blue line) and the BSA added on the fabricated electrode surface for preventing of the nonspecific binding (GP/C-dots@Ag/Cys/FA/BSA) (pink line). (C) Cyclic ECL curves of GP/C-dots@Ag (black line); GP/C-dots@Ag/Cys (red line); GP/C-dots@Ag/Cys/FA (dark blue line) and GP/C-dots@Ag/Cys/FA/BSA (light blue line).

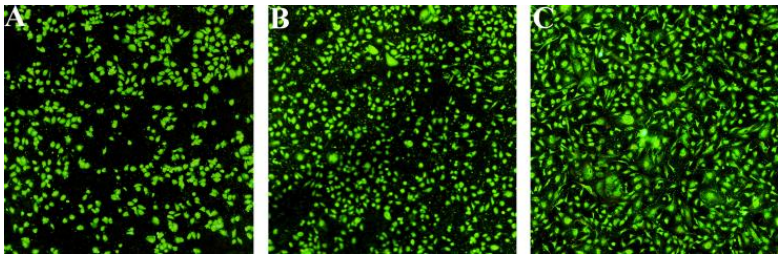

Fig. S12 Fluorescence images of HeLa cells with the concentration of 1×10^3 cells/mL cultivated on GP/C-dots@Ag/Cys/FA modified glass slides at (A) 12 h, (B) 24 h, (C) 48 h. Then stain the live cells with AO dye molecules. HeLa cells were capable of not only adhering to the film but also spreading and proliferating on the film. After incubation for 12 h, the attached round cells almost adhered and spread to irregular shapes on the surface of the film; after 48 h, the cells still had a good viability as evidenced by cell morphology and fluorescent stain by AO dye molecules. This indicates that the C-dots@Ag-modified graphene surface is noncytotoxic under our experimental conditions.

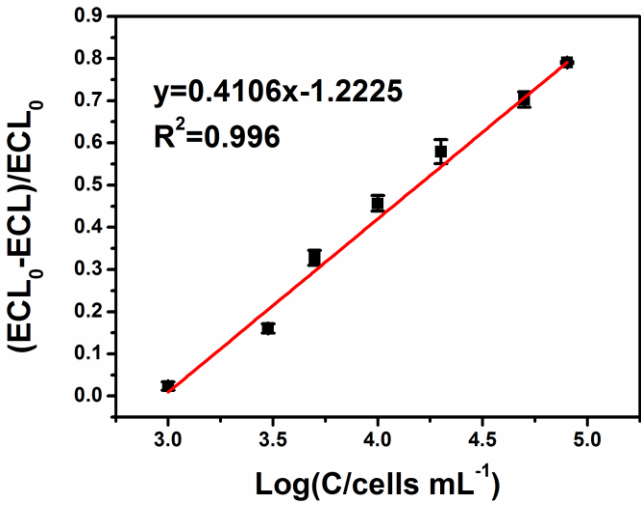

Fig. S13 The linear relationship between the degree of ECL intensity change ((ECL0-ECL)/ECL0 and logarithm of HeLa cell concentrations using C-dots@Ag/Cys/FA/BSA electrode for cytosensing.

References:

1. W. S. Hummers, R. E. Offeman, *J. Am. Chem. Soc.*, 1958, **80**, 1339.

2. Y. Song, Y. Chen, L. Feng, J. Ren, X. Qu, *Chem. Commun.*, 2011, **47**, 4436.

3. X. Wang, K. Qu, B. Xu, J. Ren, X. Qu, *Nano Res.*, 2011, **4**, 908.

4. L. Tian, D. Ghosh, W. Chen, S. Pradhan, X. Chang, S. Chen, *Chem. Mater.*, 2009, **21**, 2803.

5. Y. Li, Y. Zhao, H. Cheng, Y. Hu, G. Shi, L. Dai, L. Qu, *J. Am. Chem. Soc.*, 2012, **134**, 15.

6. L. Y. Zheng, Y. W. Chi, Y. Q. Dong, J. P. Lin, B. B. Wang, *J. Am. Chem. Soc.*, 2009, **131**, 4564.

7. Z. F. Ding, B. M. Quinn, S. K. Haram, L. E. Pell, B. A. Korgel, A. J. Bard, *Science*, 2002, **296**, 1293.

8. N. Myung, X. M. Lu, K. P. Johnston, A. J. Bard, *Nano Lett.* 2003, **4**, 183.

9. N. Myung, Y. Bae, A. J. Bard, *Nano Lett.*, 2003, **3**, 1053.

10. Y. Dong, N. Zhou, X. Lin, J. Lin, Y. Chi, G. Chen, *Chem. Mater.*, 2010, **22**, 5895.